Thermochemical Modelling of Cooled Brine Injection Into Low Enthalpy Sedimentary Reservoirs

Olga Borozdina, Thomas Ratouis, Pierre Ungemach, and Miklos Antics

GPC Instrumentation Process (GPC IP), Paris, France
olga.borozdina@geoproduction.fr • thomas.ratouis@geoproduction.fr
pierre.ungemach@geoproduction.fr • m.antics@geoproduction.fr

Keywords

Geothermal energy, water injection, fluid thermochemistry, near well bore damage, modelling, Dogger, Rijswijk sandstone

ABSTRACT

The present paper addresses the thermochemical impact of the injection of heat depleted brines into the source reservoir, exploited by means of the doublet concept of heat extraction widely used in geothermal district heating (GDH) undertakings.

Maximizing heat production requires to increase heat depletion i.e. to minimize injection temperatures. This trend is often enhanced by addition of heat pumps, a design making it possible to lower injection temperatures down to 20°C compared to the usual 40°C practiced by most grid operators.

The present work is aimed at investigating the consequences on well and reservoir performance of this strategy, whose benefits could be offset by induced thermochemical shortcomings, such as precipitation or, to the contrary, enhanced by dissolution of sensitive mineral species.

Prediction of injection-induced thermochemical behaviour was achieved by modelling rock/water interaction using two solute reactive transport software packages, SHEMAT and TOUGHREACT, applied to two case studies representative of the sedimentary, carbonate and clastic, environments hosting most GDH-eligible reservoirs.

Simulation of reactive transport kinetics tends to show that although porosity changes caused by either temperature-induced precipitation or dissolution of sensitive species (mostly calcite, anhydrite, silicates) did occur, their magnitude (hardly a few percent losses/gains) did not significantly affect porositiy neither permeability nor subsequent reservoir performance. This is likely a consequence of the fairly low temperature contrasts (≤ 50°C) in the contemplated solubility ranges.

1. Introduction

Injection of heat depleted brines into the source reservoir is a prerequisite for geothermal district heating (GDH) systems which routinely apply the doublet concept of heat mining.

This practice induces thermochemical changes, either supersaturation and precipitation or undersaturation and dissolution, of temperature-sensitive mineral species as a result of rock/water interaction. They lead ultimately to pore volume modification and either impaired (precipitation) or upgraded (dissolution) porosity/permeability patterns and related near-wellbore damage or stimulation as evidenced by positive or negative skin factors.

Maximizing heat production is currently achieved by GDH operators by increasing temperature depletion (i.e., minimizing injection wellhead temperatures). This effect is enhanced by the addition of heat pumps. Therefore, we assess the thermochemical

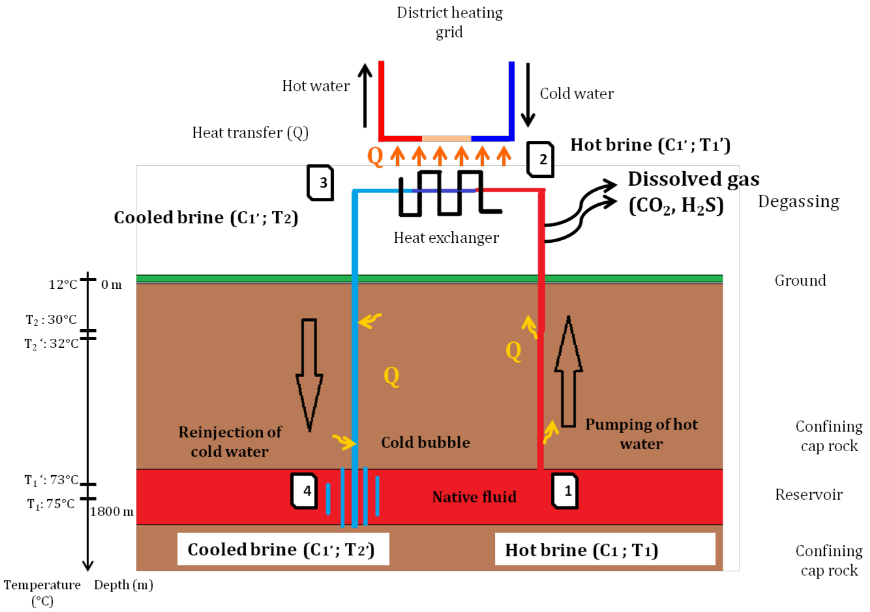

Figure 1. Geothermal district heating doublet schematic showing four fluid state changes.

impact of cooled brine injection on reservoir properties via rock/water interaction modelling.

Two case studies, contrasting carbonate and clastic sedimentary environments, were selected, and near-wellbore solute reactive transport kinetics and porosity impacts appraised by means of SHEMAT (Clauser, 2003) and TOUGHREACT (Wu et al, 2006) software.

2. Background

• *Heat Extraction*

The doublet scheme sketched in Figure1, which combines a production and an injection well, is mass balanced and heat depleted. The fluid flowing from production to injection undergoes the four thermodynamic states exemplified in Figure1, namely (i) production well bottomhole (C_1, T_1, P_1), (ii) production wellhead/heat exchanger inlet (C'_1, T'_1, P'_1), (iii) heat exchanger outlet/injection wellhead (C'_1, T_2, P_2) and, (iv) injection well bottomhole (C'_1, T'_2, P'_2), which govern fluid thermochemistry and related supersaturation/undersaturation and precipitation/dissolution key issues.

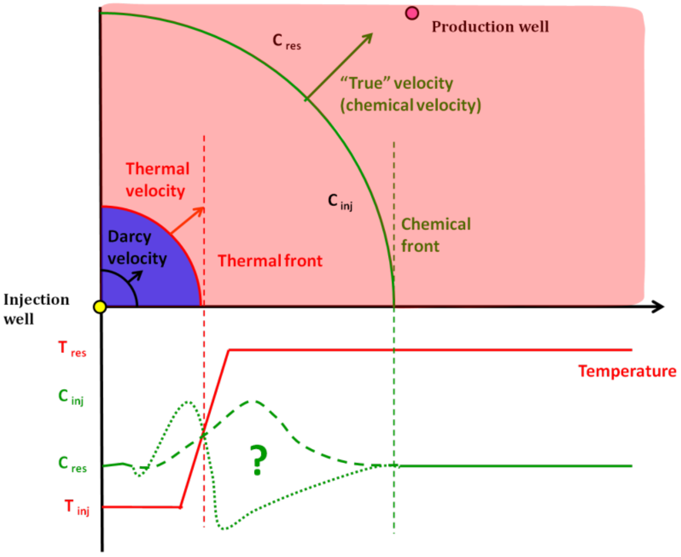

Figure 2. Injected brine; thermal vs. chemical kinetics.

Noteworthy are the contrasted thermal and chemical kinetics depicted in Figure 2 as a result of mass and heat transfers, the latter implying a heat exchange between the formation fluid and host rocks. Hence, the thermal front is delayed by a coefficient equal to the ratio of the total (rock + fluid) over the fluid heat capacities, assuming a piston convective transfer alone. This delay has obviously some implications on space and time-wise mineral concentrations.

• *Driving Processes*

They address successively (i) heat and mass transfer, (ii) temperature dependant thermochemical reactions, (iii) rock water interactions and reactive transport processes, (iv) mineral precipitation and dissolution kinetics and, (v) last but not least, porosity/permeability changes the latter appraised via the Kozeny-Carman equation.

Both Shemat (Clauser,2003) and Toughreat (Xu et al,2006) software interactively solve the mass, momentum and energy balance equations with their equations of state and boundary and initial conditions. The solute and reactive transport processes are input separately as add-ons, according to the suite described by Xu et al (2006).

• *Case Studies*

Two contrasting sedimentary environments have been selected, the Dogger carbonate reservoir in the Paris Basin (Case Study 1) and the Rijswijk sandstone aquifer in southern Netherlands (Case Study 2). Both are presently exploited and developed for district and space (greenhouse) heating purposes. Their settings are displayed in Figure 3 (Dogger limestone) and Figure 4 (Rijswijk sandstone).

Seven simulations were carried out according to injection temperature and duration as described in Table 1. Their physical, chemical and thermal characteristics are listed in Tables 2, 3 and 4. The objectives were:

- To comprehend the chemical change in the vicinity of the injection well in terms of porosity variations by analyzing the evolution of dissolved species concentrations, mineral fraction volume and porosity in terms of temperature and pH dependant amounts near the well sandface during injection (simulations 1' and A');

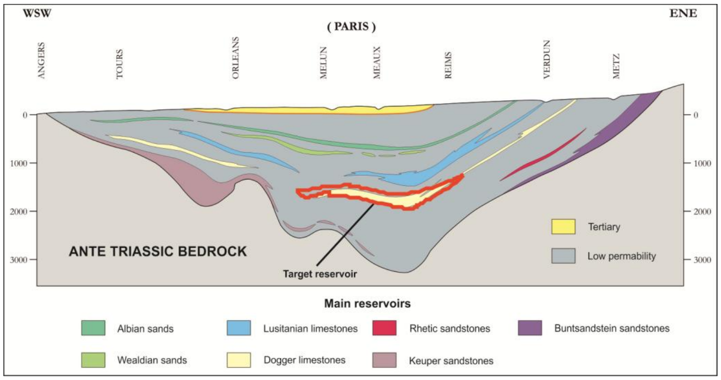

Figure 3. Case Study 1 - Dogger limestones. Cross sectional view of the Paris Basin and target reservoir (modified from Ph Maget 1983).

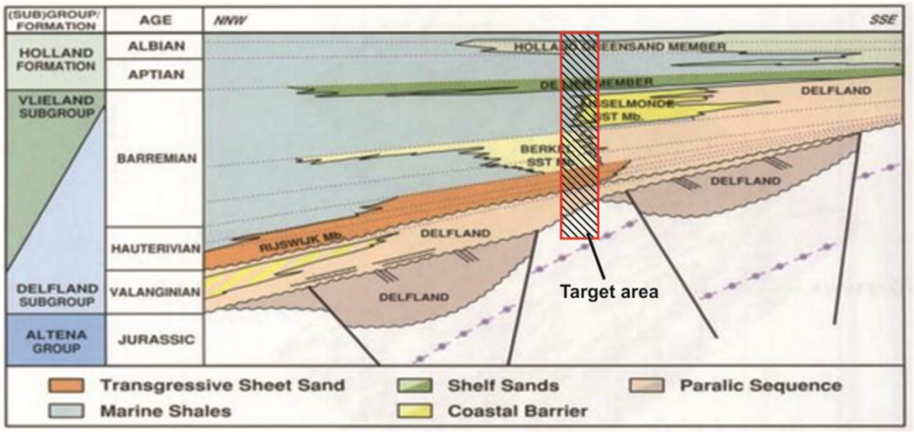

Figure 4. Case Study 2 - Rijswijk sandstones. Location of target area and geological background (Netherlands Organization for Applied Scientific Research, TNO).

- To measure the impact of temperature on porosity changes and assess optimum injection temperatures thanks to the three, temperature-wise, simulations shared by each model (simulation 1-3, A-C).

Table 1. Simulation features.

	Dogger Simulation			**Rijswijk Simulation**		
Formation Characteristics	Carbonate Rock			Sandstone		
Prevailing Minerals	**80% Carbonates** (Calcite, Dolomite) **15% Silicates** (Albite, K-Feldspar, Quartz) **5% Anhydrite**			**92.6% Silicates** (Albite, K-Feldspar, Quartz, Kaolinite) **7.4% Carbonates** (Calcite, Dolomite)		
Simulation Time	50 days ' / 20 years					
Space Discretization	[2m - 512m]					
Simulation Name	B	A' / A	C	2	1' / 1	3
Temperature (°C)	20	30	40	20	30	40

Table 2. Hydraulic and thermal parameters.

Feature	**Settings**	
	Productive Layer	Confining Layer
Thickness [m]	10	95
Initial porosity, [-]	0.15	0.01
Initial permeability, [m^2]	3.5 .10^{-12}	10^{-18}
Rock density, [k.m^{-3}]	2700	
Thermal conductivity, [W m^{-1} K^{-1}]	2.5	2.2
Formation temperature, [°C]	75	
Formation pressure [Pa]	180.10^5	
FLOW Well [kg.s^{-1}]	Constant hydraulic head 33.3	
Specific Heat [J.kg^{-1}]	1100	1100

Table 4. Host rock composition and characteristics.

Minerals		**Chemical Formulae**	**Grain Radius (m)**	**Surface Area (cm²/g)**	**Volume Fraction (%)**	
					Dogger	**Rijswijk**
Carbonates	calcite	$CaCO_3$	0.001	9.8	70	1.2
	dolomite	$(Mg, Ca)CO_3$			10	6.2
Silicates	quartz	SiO_2			5	61.4
	albite	$NaAlSi_3O_8$			5	9.8
	Kfeldspar	$KAlSi_3O_8$			5	9.2
	kaolinite	$Al_2Si_2O_5(OH)_4$				12.2
Sulfide Mineral	anhydrite	$CaSO_4$			5	

3. Results

3.1. Temperature Transients

Due to the delayed thermal front displacement (Figure 2), the reservoir, during cooled brine injection, will be first affected by any fluid chemical change and later undergo temperature depletion.

Table 3. Native fluid concentrations.

Aquifer		**Dogger**	**Rijswijk**
Element		Concentration (mol/L)	
Aluminium	Al	3.385E-07	5.9E-8
Boron	B	1.631E-03	
Barium	Ba	3.635E-07	
Bromine	Br	9.608E-04	
Calcium	Ca^{2+}	5.241E-02	1.63E-1
Chlorides	Cl^-	5.394E-01	1.82E-3
Fluorine	F	3.262E-05	
Iron	Fe	1.071E-04	
Hydronium	H_3O^+	7.99E-06	1.36E-04
Bicarbonates	HCO_3^-	4.292E-03	9.65E-4
Potassium	K^+	3.77E-03	9.2E-3
Lithium	Li	3.733E-04	
Magnesium	Mg^{2+}	2.656E-03	7.1E-3
Manganese	Mn^{2+}	1.100E-06	1.78E-5
Sodium	Na^+	4.350E-01	1.42
Nitrate	NO_3^-	1.523E-03	
Silica	$SiO_{2\,(aq)}$	6.202E-04	5.22E-4
Sulfates	SO_4^{2-}	1.085E-02	1.57E-3
Strontium	Sr^{2+}	6.680E-04	4.12E-3

3.2. Chemical Processes

3.2.1. Reaction Kinetics - Case Study 1

During cold brine injection, four different assemblages, each accounting for three consecutive processes, either pH (via the chemically imbalanced fluid) or temperature (via the thermal front arrival) controlled, can be identified in the vicinity of the injection well.

• *In Situ Imbalance*

1. The injected fluid is cooled to 30°C; therefore, it is not at equilibrium. When cold fluid injection starts, an immediate and abrupt change in geochemical parameters is noticed, which affects:
    - pH,
    - most dissolved element concentrations, and,
    - concerned minerals (composed of these elements) such as calcite, dolomite and anhydrite.

It reflects the establishment of a new cooled fluid equilibrium.

• *Temperature Front Impacts*

2. Cold water reaches the observation point 30m distance from the injection well. The thermal front disturbs the newly set equilibrium. No new equilibrium is established during the present phase since both dissolved species and mineral concentrations share the same trend. It is a transitory stage.
3. As temperature declines, it will affect the solubility product of the mineral dissolution reaction. Below a given (mineral dependent) temperature this effect will prevail. The geochemical system trends towards a new equilibrium state,

as dissolved species concentrations are compensated by mineral precipitation.

4. Finally, temperature stabilizes, coinciding with element concentration stabilization; however mineral precipitation or dissolution continues, meaning that the geochemical system assembling these elements, has not yet reached equilibrium.

To illustrate these mechanisms, time-dependent graphs are presented. They illustrate the time dependant evolution of different parameters (temperature, pH, concentration of dissolved elements and changes in mineral concentrations) at an observation point 30m distance from the injection well.

As shown in Figures 5 to 8, the system exhibits the four different assemblages during cold fluid injection, summarised as follows:

- Assemblage 1. Before any temperature change, the geochemical system undergoes sudden changes:
  - A pH rise from 5.33 to 5.78,
  - Dissolved ions [Ca2+], [Mg2+] and [SO42-] concentrations decline,
  - Positive changes in Anhydrite (CaSO4), dolomite [(Ca, Mg) (CO3)2] and Calcium-composed minerals (carbonates + anhydrite) concentrations. Silicates do not seem to experience such change in concentration, indicative of (very) slow reaction kinetics.

  The in-situ fluid imbalance causes either a rise or a fall of the dissolved element concentration that is compensated by either an increase or decrease of the corresponding mineral concentrations to reach a new equilibrium.
- Assemblage 2 reflects the arrival of the thermal front. Graphs have shown that while temperature decreases, the geochemical system evolves without reaching a new equilibrium. pH rises, calcium, magnesium and sulphate concentrations alike. Anhydrite, dolomite and Calcium-composed minerals concentrations progressively increase. Silica and Silica-composed minerals (silicates) trend opposite. It can be assumed that, as the cold fluid replaces the fluid in place, it disrupts the equilibrium and induces super or under saturation. The foregoing suggests that further research be undertaken to fully comprehend the phenomenology.
- Assemblage 3 starts when temperature reaches a temperature threshold below which its impact on equilibrium constants seems to prevail. It appears that Anhydrite, dolomite and Calcium-composed minerals experience a solubility rise, thus rendering the system undersaturated and favoring dissolution of sulfate-magnesium-calcium minerals. Conversely, silicates solubility drops, causing the system to become supersaturated and silicates to precipitate.

Accordingly, when temperature declines, a retrograde solubility effect (solubility rise) is noticed for Calcium-composed minerals, Calcium ion concentration increases. On the contrary Silica-composed minerals solubility decrease, aqueous Silica concentration decreases, which conforms to a prograde solubility, behaviour highlighted in Figure 9.

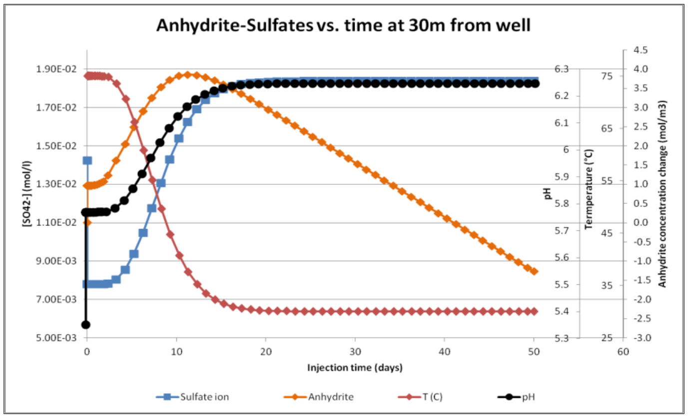

Figure 5. Simulation A. Time dependent Sulfate (SO_4^{2-}) and Anhydrite ($CaSO_4$) concentrations vs. pH and temperature.

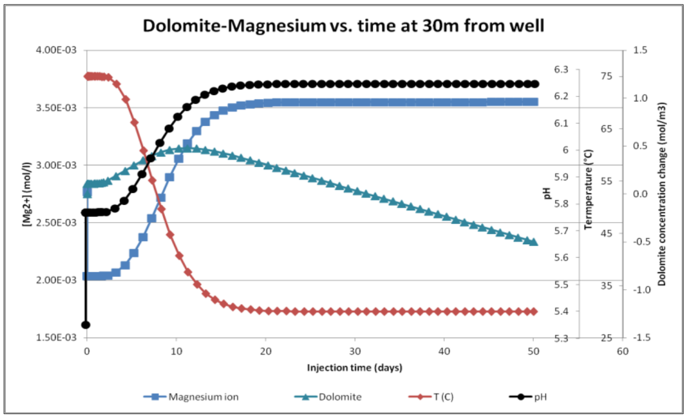

Figure 6. Simulation A. Time dependent Magnesium (Mg^{2+}) and Dolomite ($(Mg,Ca)(CO_3)_2$) concentrations vs. pH and temperature.

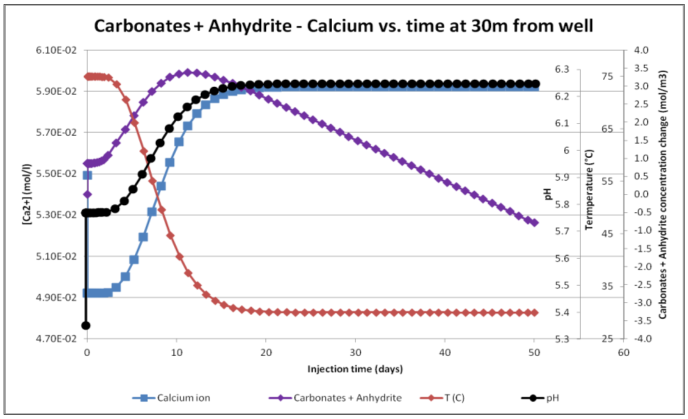

Figure 7. Simulation A. Time dependent Calcium (Ca^{2+}), Calcite ($CaCO_3$), Dolomite ($(Mg,Ca)(CO_3)_2$) and Anhydrite ($CaSO_4$) concentrations vs. pH and temperature.

- Assemblage 4 is initiated when temperature stabilizes. It is characterized by constant pH and solute concentrations. However, the system has not yet reached equilibrium as precipitation/dissolution of minerals are ongoing; the system tends towards equilibrium.

  Chemical changes in the reservoir affect its hydrogeological performance. This is illustrated in Figures 10 and 11

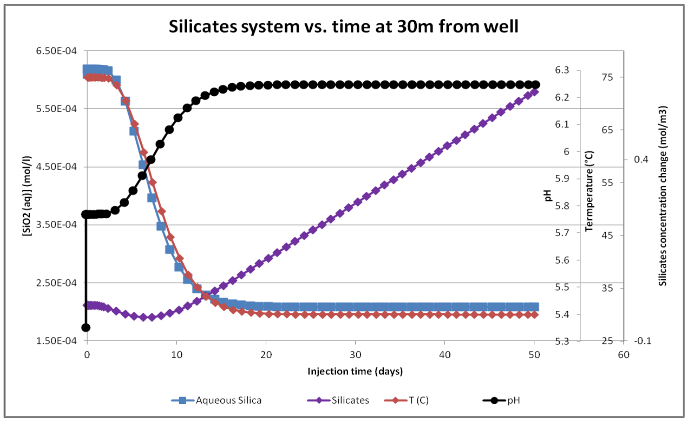

Figure 8. Simulation A. Time dependent Silica ($SiO_{2\ (aq)}$), Quartz (SiO_2), K-Feldspar ($KAlSi_3O_8$) and Albite ($NaAlSi_3O_8$) concentrations vs. pH and temperature.

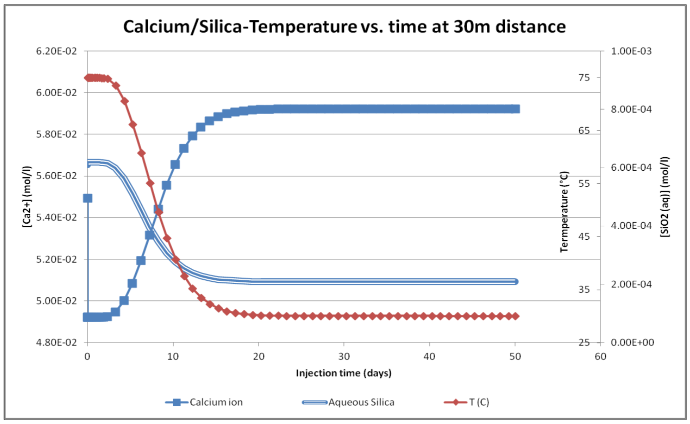

Figure 9. Case Study 1. Simulation A. Temperature impact on Calcium (Ca^{2+}) and Silica ($SiO_{2\ (aq)}$) solubilities.

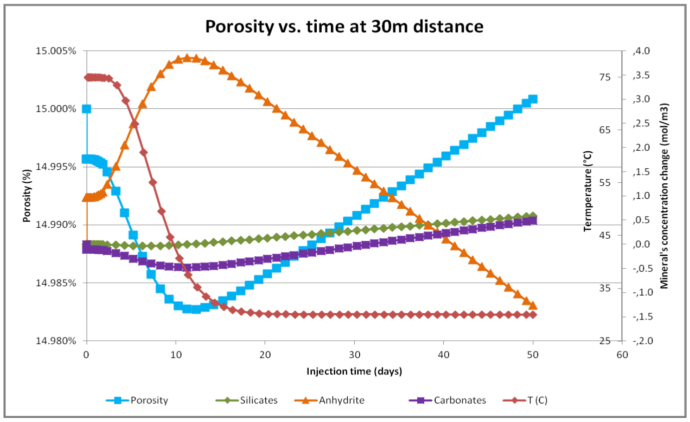

Figure 10. Case Study 1. Simulation A. Porosity and mineral concentration changes vs. injection time.

where porosity changes are plotted against temperature, distances to the well sandface and changes in concentration of selected minerals.

It can be seen that carbonates and silicates tend to slightly reduce porosity over time. Porosity is more affected by anhydrite dissolution. Nevertheless, after 50 days injection, porosity in the immediate vicinity of the well increases only 0.12%, and loses no more than 0.03% at 60m, which is insignificant with respect to permeability changes.

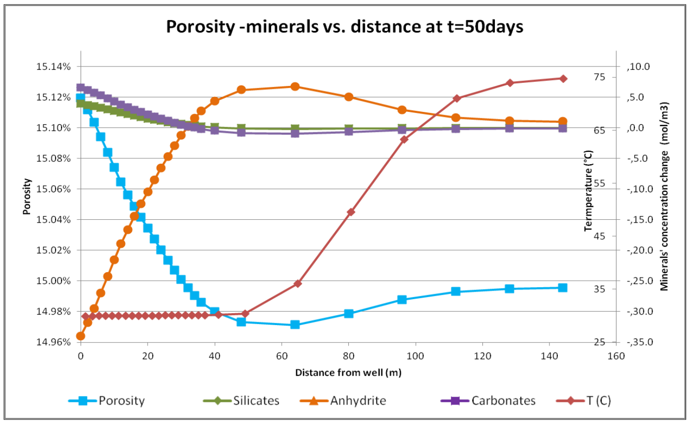

Figure 11. Case Study 1. Simulation A. Porosity and mineral concentration changes vs. distance.

3.2.2. Reaction Kinetics - Case Study 2

The Rijswijk sandstone reservoir trends similar to the Dogger aquifer. The same four assemblages can be identified during cooled brine injection.

Nevertheless, there are several differences between the two models, listed hereunder:

- The fluid never gets undersaturated with respect to silica, as no dissolution is observed.
- During phase two, calcium concentration increase is immediately compensated by a drop in carbonate concentrations. Therefore, it seems that kinetics of calcite precipitation is higher than that of other species, thus enabling the calcium system to tend more rapidly toward equilibrium.
- The most remarkable difference between the two models addresses the absence of anhydrite in the Rijswijk Sandstone. In Simulation A, porosity changes are mainly attributed to anhydrite dissolution/precipitation. Near the wellbore, massive anhydrite dissolution enhances reservoir porosity. In Simulation 1, the lack of anhydrite prevents this effect. Moreover, in both models, carbonates and silicates display the same behaviour, precipitating near the well sandface during injection.

3.3. Long Term Reservoir Response

3.3.1. Porosity Change After 20 Years of Cooled Brine Injection

- Case Study 1

Figure 12 depicts the porosity and mineral concentration changes after 20 years of cooled brine injection into the Dogger aquifer. Each simulation (B, A, C) follows the same general trend. Only do magnitudes vary. The lower the final temperature, the higher the changes (the geochemical system standing far away from the initial equilibrium).

Moreover it shares the same trend described previously i.e. continuous dissolution and precipitation reactions, confirming that a new equilibrium has not yet been reached.

Nevertheless, the important variation of break in the anhydrite concentration slope indicates that either the anhydrite geochemical system gets close to a new equilibrium (slower chemical reactions) or that almost all the anhydrite has been dissolved. It therefore implies that a sharp porosity drop occurs near the wellbore, which increases with decreasing injection temperatures.

- Case Study 2

Figure 13 shows the porosity and mineral concentration changes after 20 years of cooled brine injection into the Rijswijk sandstone aquifer. It can be noticed a 2% porosity increase occurs, reaching a plateau at 600m from the well.

3.3.2. Summary of Porosity Transients

Figure 14 and Table 5 summarises the porosity changes for both models after 20 year continuous injection. Opposite responses to cooled brine injection, one apparent with a porosity increase for the Rijswijk sandstone (Case Study 2), and a porosity decrease for the Dogger limestone (Case Study 1). Porosities elsewhere stabilize at 600m from the injection well; otherwise, the lower the injection temperature, the higher the contrast in porosity changes.

4. Discussion

Reservoir petrography and simulation results are summarised in Table 5, and suggest the following comments:

a) Carbonate Rocks

Maximum porosity gains and losses amount, after twenty years continuous injection, to about 4% and to 0.25% at 16 and 300 m from the well face, respectively. Near wellbore porosity increase reflects a prevailing anhydrite dissolution which affects almost the whole mineral assemblage, although it contributes only 5% of the rock mass, whereas calcite (retrograde) solubility contribution is minimal.

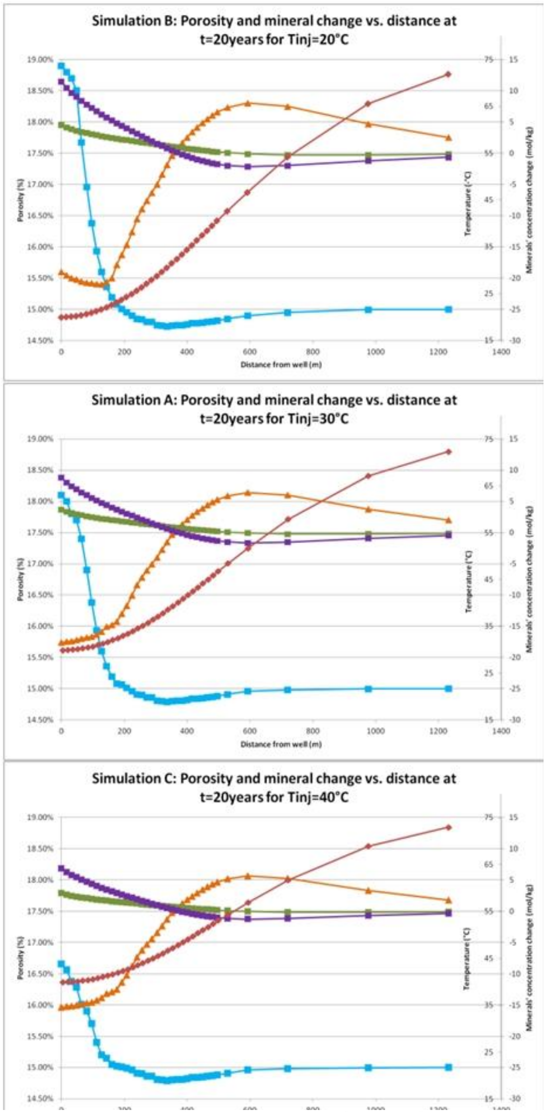
Simulation B: Porosity and mineral change vs. distance at t=20years for Tinj=20°C

Simulation A: Porosity and mineral change vs. distance at t=20years for Tinj=30°C

Simulation C: Porosity and mineral change vs. distance at t=20years for Tinj=40°C

Figure 12. Case Study 1 - Porosity and mineral concentration vs. time, distance and injection temperature after 20 year injection.

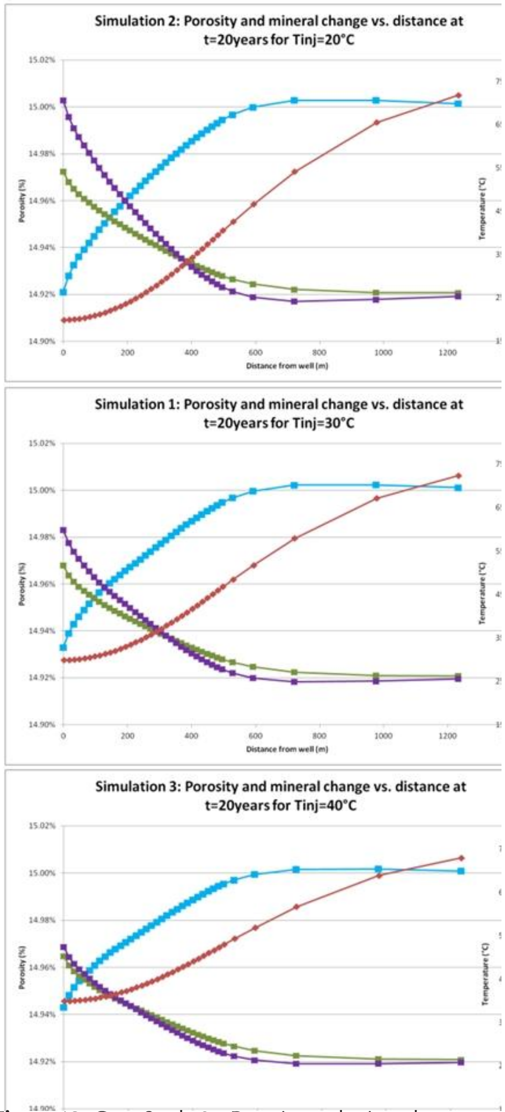
Simulation 2: Porosity and mineral change vs. distance at t=20years for Tinj=20°C

Simulation 1: Porosity and mineral change vs. distance at t=20years for Tinj=30°C

Simulation 3: Porosity and mineral change vs. distance at t=20years for Tinj=40°C

Figure 13. Case Study 2 - Porosity and mineral concentration vs. time, distance and injection temperature after 20 year injection.

b) Sandstone Matrix

Here the thermochemical behaviour is opposite to that of the carbonate reservoir. Maximum porosity increases, limited to 0.15%, are noticed at 800m from the wellbore and higher losses, amounting to 2%, close to the well sandface, are logically attributed to increased silicates solubility.

c) Near Wellbore

As previously noted, a lower injection temperature produces larger changes in porosity.

d) Modelling

Owing to a single injection well configuration, modelling does not accurately reflect the actual doublet pressure/temperature patterns, in spite of partly compensating boundary conditions set at constant pressure. Consequently, results at greater distances from the well ought to be regarded cautiously. Near-wellbore results, however, are deemed mostly reliable and should not be questioned.

5. Conclusion

The ability to predict the chemical behaviour of the formation fluid during the exploitation cycle is raising a growing interest among geothermal operators be-

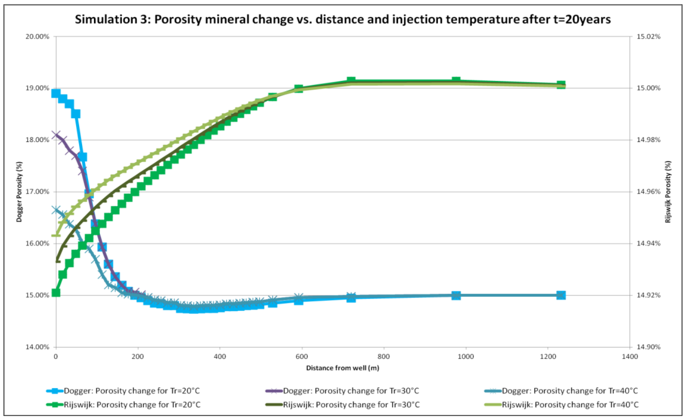

Figure 14. Intercomparison of overall porosity transients.

Table 5. Summary sheet. Simulation input data and output results.

Aquifers		**Dogger**			**Rijswijk**		
Formation characteristics		Carbonate rock			Sandstone matrix		
Prevailing minerals		Carbonates			Silicates		
Simulation run name		B	A	C	2	1	3
Injection temperature (°C)		20	30	40	20	30	40
Maximum porosity	Distance from well (m)	16	16	16	800	800	800
	Value	0.1895	0.181	0.167	0.1515	0.1508	0.1505
	Gain (%)	3.95%	3.1%	1.7%	0.15%	0.08%	0.05%
Minimum porosity	Distance from well	300	300	300	16	16	16
	Value	0.1475	0.148	0.1485	0.13	0.1338	0.136
	Loss (%)	0.25%	0.2%	0.15%	2%	1.62%	1.4%
Porosity gain/loss in the immediate vicinity of the injection well		+3.95%	+3.1%	+1.7%	-2%	-1.62%	-1.4%

cause injection has become a mandatory practice, and low injection temperature necessary to maximize energy output.

However, necessary to maximize injecting heat-depleted brine into the source reservoir, may result in thermochemical shortcomings. Geochemical solute transport modelling is therefore required to provide operators and technologists with relevant preventative, remedial and design procedures.

Bearing in mind these concerns, the present work focused on predicting injection-induced thermochemical trends, and eventual well and formation damage. TOUGHREACT and SHEMAT software packages were used to assess geochemical changes in response to decreasing temperatures.

Two case studies address low enthalpy carbonate (Dogger limestone, Paris Basin) and clastic (Rijswijk sands and sandstones, South Netherlands Basin) sedimentary reservoir environments. The practical outcome of these simulations indicates that, although porosity changes caused by temperature-induced precipitation or dissolution of mineral species (carbonates, anhydrite, silicates) do occur. However, their magnitude (hardly a few percent losses/gains) does not significantly alter, within the contemplated moderate temperature/solubility ranges, porosities neither permeabilities nor subsequent reservoir performance.

Future work will supply the foregoing methodology to the simulation of the whole doublet and multidoublet GDH systems.

References

Borozdina O., P. Ungemach, and M. Antics, 2011. “Near well geochemical impact of cooled geothermal brine injection. Application to selected sedimentary reservoir environments.” 1st Sustainable Earth Sciences Conference and Exhibition. Technologies for Sustainable use of Deep Sub-surface. 8-11 November 2011, Valencia, Spain.

Castillo C., and al. 2011. **“**Assessing the Geochemical Impact of Injection of Cooled Triassic Brines into the Dogger Aquifer (Paris Basin, France): A 2D Reactive Transport Modeling Study.” BRGM/SGP-TR-191. 2011.

Clauser C., 2003. “Numerical Simulation of Reactive Flow in Hot Aquifers. SHEMAT and Processing SHEMAT,” Springer. User’s guide.

Kühn M., W. Schneider. (2003). “Injection Well with Reaction Kinetics. Clauser C (ed) Numerical simulation of reactive flow in hot aquifers - SHEMAT and Processing SHEMAT”, Springer Publishers, Heidelberg, 253-262.

Ratouis T., (2012). “Study of fluid-rock interaction during geothermal injection. Case studies. GPC IP open file report DCE12036”. Roissy en France.

Rojas J., (Editor),1989. “Caractérisation et Modélisation du Reservoir du Dogger, Bassin Parisien, France. *Rapport Final*.” R & D Contract EN3G-0046-F (CD). European Commission, Brussels, Belgium.

Sperl J., and J. Trckova, 2008. “Permeability and porsosity of rocks and their relationship based on laboratory testing.” Institute of Rock Structure and Mechanics, Academy of Science of the Czech Republic, Prague, Czech Republic.

Ungemach P., 2003. Reinjection of cooled geothermal brines into sandstone reservoirs. *Geothermics*, v. 32, p. 743-761.

Ungemach P., M. Antics, and M. Papachristou, 2005. **“**Sustainable Geothermal Reservoir Management.” *Proceedings* World Geothermal Congress 2005.

Xu, Tianfu, and al. 2006. “TOUGHREACT User’s Guide: A Simulation Program for Nonisothermal Multiphase Reactive Geochemical Transport in Variably Saturated Geologic Media”. Earth Sciences Division, Lawrence Berkeley National Laboratory University of California, Berkeley, CA 94720/ LBNL-55460. 2006. User’s Guide.